We are IntechOpen,
the world's leading publisher of
Open Access books
Built by scientists, for scientists

**4,800**
Open access books available

**122,000**
International authors and editors

**135M**
Downloads

Our authors are among the

**154**
Countries delivered to

**TOP 1%**
most cited scientists

**12.2%**
Contributors from top 500 universities

BOOK CITATION INDEX
CLARIVATE ANALYTICS
INDEXED

**WEB OF SCIENCE**™

Selection of our books indexed in the Book Citation Index
in Web of Science™ Core Collection (BKCI)

Interested in publishing with us?
Contact book.department@intechopen.com

Numbers displayed above are based on latest data collected.
For more information visit www.intechopen.com

# Fluctuations of Stiff Polymers and Cell Mechanics

Jens Glaser and Klaus Kroy
*Leipzig University*
*Germany*

> Indeed, the vista of the biochemist is one with an infinite horizon. And yet, this program of explaining the simple through the complex smacks suspiciously of the program of explaining atoms in terms of complex mechanical models.
>
> *Max Delbrück*

## 1. Introduction

Understanding complex systems through the study of minimal models that capture their underlying universal principles has always been the tradition of physics. This reductionist approach is challenged by the vast complexity of life and the accumulating knowledge in molecular biology. Biological sciences have always laid an emphasis on diversity rather than on simplicity and universality. And rightly so, since diversity is a sine qua non of evolutionary robustness and adaptability (Kirschner & Gerhart, 1998). Bearing in mind this tension, the insight that cellular functions can be attributed to functional modules (Hartwell et al., 1999) as a higher level of biological organization offers a new perspective on a possible unification of the two seemingly contradictory paradigms. It stimulated the emergence of "bottom-up approaches" (Bausch & Kroy, 2006; Schwille & Diez, 2009; Liu & Fletcher, 2009) aiming at the reconstitution of functional modules of cell biology *in-vitro*. The reconstitution of a simplified biological system with a reduced number of components mutually depends on a detailed level of physical understanding, reveals how evolved biological systems work and provides insight into how new biological functions could be engineered.

Cellular mechanics represents an important example for the application of this idea (Bao & Suresh, 2003; Discher et al., 2009; Fletcher & Mullins, 2010). The bottom-up approach to cell mechanics has revealed the basic mechanisms underlying the complex mechanical behavior of the eukaryotic cytoskeleton (Fig. 1, left) by reconstituting self-assembling networks of biopolymers *in-vitro* in an attempt to balance the mutually conflicting demands for simplicity and complexity (Fig. 1, middle) (Bausch & Kroy, 2006).

The present contribution adopts the coarse-graining approach tested in polymer physics and explores how far it takes us in the task of understanding the functional modules responsible for cellular mechanics. We progress from a minimal model for single semiflexible polymers to a theoretical description of their complex networks. It turns out that on this basis many crucial features found in experimental studies of cellular mechanics can be understood qualitatively if not quantitatively. Semiflexible polymers are characterized by their persistence length $\ell_p$, which is a mesoscopic length scale, much larger than the microscopic
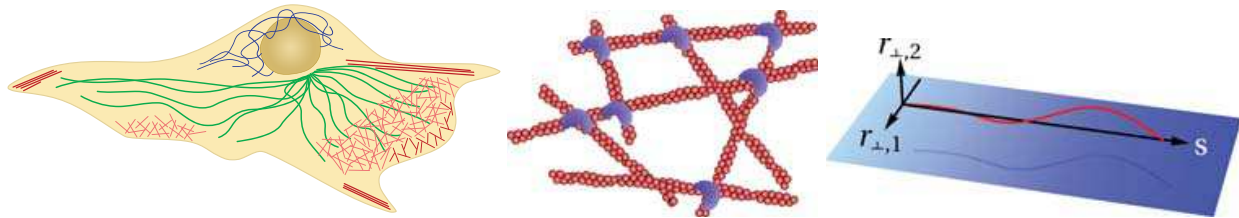
Fig. 1. Bottom-up approach to cell mechanics. *Left:* Schematic view of the cytoskeleton of the eukaryotic cell, showing microtubules (green), actin stress fibers and networks of the cortex and lamellipodium (red), and intermediate filaments (blue). *Middle:* A reconstituted actin network crosslinked by actin-binding proteins. *Right:* A single semiflexible filament described by a mathematical minimal model, the wormlike chain.

monomer length. It indicates the backbone length over which thermal fluctuations bend the polymer significantly, and microscopically, it arises from the backbone's finite bending stiffness, as described mathematically by the wormlike chain (WLC) model (Fig. 1, right).

Double-stranded DNA is a prototypical semiflexible polymer (Bustamante et al., 2003) with a persistence length of $\ell_p \approx 50$nm that has been measured by single-molecule stretching experiments. The protein machinery for transcription and replication of DNA is highly adapted to the mechanical stiffness of DNA. Also, mechanical bending energy is required to wind DNA into a tightly packed conformation in the nucleosome.

As another important example, the semiflexible protein filaments of the cytoskeleton provide the structural basis of cellular mechanics. The cytoskeleton of the eukaryotic cell consists of three major classes of semiflexible filaments: microtubules, F-actin and intermediate filaments (see Fig. 1, left). In the cell, these filaments form self-assembling networks.

Microtubules are the most rigid of the cytoskeletal polymers with persistence lengths on the order of millimeters, and they are capable of bearing significant compressive load. They form a star-like network that spans the cell, which allows them to act as rails for intracellular transport. During cell division, this network transforms into a bipolar structure (the mitotic spindle) separating the DNA into two identical sets.

Filamentous (F-)actin is a biopolymer protein with $\ell_p \approx 10\mu$m (Isambert et al., 1995) assembled from globular (G-)actin monomers, which are of macromolecular size themselves. The actin cortex is a thin, membrane-bound F-actin network that is employed to maintain and transform the cell's shape. Lamellipodia, filopodia and microvilii are actin-rich structures, and polymerization-dependent forces push these cellular protrusions out of the cell. In muscles, actin provides tracks along which myosin motors walk to generate contractility.

The third type of cytoskeletal polymers, rope-like intermediate filaments, comprises a group of different biopolymer families, which are relatively flexible ($\ell_p \approx 1\mu$m) (Schopferer et al., 2009; Lin et al., 2010) and much less is known about their role in cell mechanics than for actin filaments and microtubules. Intermediate filaments lend mechanical support to the nuclear envelope. In the cytoplasm, a network of intermediate filaments helps the cell to resist shear stress.

In the cell, all three types of protein networks intertwine and interact. For example, the buckling resistance of microtubuli is enhanced by the lateral constraints provided by the surrounding actin and intermediate filament meshworks (Brangwynne et al., 2006), providing a natural paradigm for fiber-reinforced materials, which are also very popular in engineering.

In the following, we review the WLC model and its properties in thermal equilibrium and we infer salient predictions for the dynamics of single semiflexible polymers (Sec. 2). Recent results for their non-equilibrium dynamic response to stretching forces are briefly summarized. Subsequently, we address biopolymer networks *in-vivo* and *in-vitro* and review experimental results that were obtained using the bottom-up approach to cell mechanics (Sec. 3). Theoretical concepts for the description of semidilute solutions of WLCs are introduced. We review theories of the tube and its heterogeneities (Sec. 4), and models of crosslinked biopolymer networks (Sec. 5). Finally we provide a brief overview of models of the viscoelastic and inelastic dynamics of stiff polymer solutions and networks (Sec. 6).

## 2. Fluctuations and response of wormlike chains

We begin by introducing the mathematical minimal model of a semiflexible polymer, the wormlike chain (WLC). Historically, the concept of a semiflexible polymer that bends only on scales much larger than the monomer size was introduced to explain scattering experiments on thread-like molecules (Kratky & Porod, 1949). The description of a semiflexible polymer as a finitely extensible, differentiable space curve with a curvature energy was introduced in the framework of statistical mechanics by Saitô et al. (1967). We will henceforth refer to it as the WLC. This has become a standard model of polymer physics (Yamakawa, 1971; Doi & Edwards, 1988), and, in the context of biopolymers, it has been useful for the analysis of dynamic light scattering data of F-actin solutions (Farge & Maggs, 1993; Kroy & Frey, 1997). In particular, the simple analytical interpolation formula for the non-linear force-extension relation of a WLC proposed by Marko and Siggia explains force spectroscopy experiments with DNA (Bustamante et al., 1994; Marko & Siggia, 1995) and has led to a surge of applications in single-molecule experiments. Moreover, the WLC enters theories for polymers in confinement (Odijk, 1983; Semenov, 1986; Morse, 2001), under the application of forces (MacKintosh et al., 1995; Kroy & Frey, 1996; Seifert et al., 1996; Hallatschek et al., 2005), compressive load (Baczynski et al., 2007; Emanuel et al., 2007), under shear (Gittes et al., 1997; Morse, 1998c) or in flow fields (Morse, 1998b; Munk et al., 2006), for their bundles (Heussinger et al., 2007) or rings (Alim & Frey, 2007; Ostermeir et al., 2010). The WLC model has been used to characterize a wide range of other biological macromolecules besides DNA and cytoskeletal polymers, including muscle proteins (Tskhovrebova et al., 1997), RNA (Caliskan et al., 2005) or polysaccharides (Vincent et al., 2007).

In the following, we first concentrate on the fluctuations of single wormlike chains and their response to stretching forces, then we extend the picture to include the equilibrium and non-equilibrium dynamics.

### 2.1 Equilibrium properties of the WLC
### 2.1.1 Definition and basic properties

The WLC model represents the semiflexible polymer of contour length $L$ by a differentiable space curve $\mathbf{r}(s)$ (see Fig. 1, right) with a curvature energy

$$\mathcal{H}_{WLC} = \frac{\kappa}{2} \int_0^L \mathrm{d}s \left[ \mathbf{r}''(s) \right]^2 , \qquad (1)$$

where $\kappa$ denotes the bending rigidity, together with the (local) constraint of inextensibility

$$|\mathbf{r}'(s)| = 1. \tag{2}$$

Thermal averages are defined with respect to this Hamiltonian via a functional integral

$$\langle \ldots \rangle \equiv \int \mathcal{D}\mathbf{r}(s)\,\Psi[\mathbf{r}(s)]\ldots,$$

where

$$\Psi[\mathbf{r}(s)] \propto \delta\left\{\left[\mathbf{r}'(s)\right]^2 - 1\right\}\exp\left(-\frac{\mathcal{H}_{WLC}}{k_B T}\right)$$

is the statistical weight associated with the WLC Hamiltonian. The persistence length $\ell_p = \kappa/k_B T$ (in $d=3$) emerges as the correlation length of the exponential decay of contour tangents in thermal equilibrium, i.e.,

$$\langle \mathbf{t}(s)\mathbf{t}(s') \rangle = \exp\left(-\frac{|s - s'|}{\ell_p}\right), \tag{3}$$

with $\mathbf{t}(s) \equiv \mathbf{r}'(s)$. Eq. (3) follows from the formal equivalence between the statistical weight $\Psi[\mathbf{r}(s)]$ of a WLC conformation, expressed in terms of the tangent orientation $\mathbf{t}(s)$, and the Wiener measure for diffusion on the surface of the unit sphere $|\mathbf{t}| = 1$ (Landau & Lifshitz, 1980; Doi & Edwards, 1988). As a direct consequence of the tangent-tangent correlations, the mean-square end-to-end distance $\langle R^2 \rangle$ of a WLC approaches the following asymptotic limiting cases, depending on the ratio of $L$ to $\ell_p$:

$$\langle R^2 \rangle \to \begin{cases} L^2 & \ell_p \gg L \quad \text{(rigid rod)} \\ 2\ell_p L & \ell_p \ll L \quad \text{(flexible polymer).} \end{cases}$$

Thus, the persistence length demarcates cross-over from rigid rod behavior on short scales to flexible phantom chain (or random walk) behavior on large scales, where the effective step size or "Kuhn length" is $2\ell_p$.

### 2.1.2 Transverse fluctuations - the weakly bending rod

In many applications, semiflexible polymers are almost straight over the length scales of interest, either because of their intrinsic stiffness or because they are stretched by external forces. Thus, loops and overhangs of the contour are unlikely. In the weakly-bending rod (WBR) approximation the contour is parametrized by two-dimensional excursions $\mathbf{r}_\perp(s)$ transverse to a preferred axis lying along the longitudinal or $\parallel$-direction (as shown in Fig. 1, right),

$$\mathbf{r}(s) = [\mathbf{r}_\perp(s), s - r_\parallel(s)].$$

Here, $s - r_\parallel(s)$ is the coordinate along the preferred axis, and the quantity $r_\parallel(s)$ with $r'_\parallel(s) \ll 1$ is called the projected (or stored) length, referring to the contour length stored in the transverse undulations. Thus, for a stiff polymer the local arc-length constraint $|\mathbf{r}'(s)| = 1$ (Eq. (2)) is expanded as

$$r_\parallel'(s) \approx \frac{1}{2}\left[\mathbf{r}_\perp'(s)\right]^2 + \mathcal{O}[(\mathbf{r}_\perp')^4], \qquad (4)$$

to leading order in the small transverse components $\mathbf{r}_\perp'$ of the contour tangent.

For a WBR, the exponential decay of the tangent correlations of a free WLC noted in Eq. (3) amounts to a diffusive growth of the mean-square displacement (MSD) of the transverse tangent vector as a function of the arc-length separation, $\langle[(\mathbf{r}_\perp'(s) - \mathbf{r}_\perp'(0)]^2\rangle = 2|s|/\ell_p$. For a WLC grafted at one end ($s = 0$) with $\mathbf{r}_\perp(0) = \mathbf{r}_\perp'(0) = 0$, the mean square transverse fluctuations are therefore calculated as

$$\langle\mathbf{r}_\perp^2(s)\rangle = \frac{2s^3}{3\ell_p}, \qquad (5)$$

which can be interpreted as a roughness relation for the (asymptotically) self-affine contour fluctuations of the thermally agitated WBR.

### 2.1.3 Asymptotic distribution of end-to-end distances

An important quantity distinguishing a stiff polymer from a flexible one is the probability distribution $P(\mathbf{r}) \equiv \langle\delta[\mathbf{r} - \mathbf{R}]\rangle$ of the end-to-end-vector $\mathbf{R} \equiv \mathbf{r}(L) - \mathbf{r}(0)$. For flexible chains such as the freely-jointed chain, it is exactly known and for many purposes approximated well by a Gaussian centered around $\mathbf{r} = \mathbf{0}$ (Yamakawa, 1971). Stiff polymers behave drastically different, since their distribution $P(\mathbf{r})$ exhibits a peak near full extension. We quote here the exact asymptotic result for the $P(\mathbf{r})$ of a WBR from Wilhelm & Frey (1996).

$$P(\mathbf{r}) \sim \frac{\mathcal{N}}{x^{3/2}}\left(\frac{1}{x} - 2\right)\exp\left(-\frac{1}{4x}\right), \qquad x = \frac{\ell_p}{L}(1 - r/L). \qquad (6)$$

This is the leading term of an infinite series for $P(\mathbf{r})$ and it is valid near full extension, i.e. for $1 - r/L \ll L/\ell_p$. The radial distribution function, obtained from $P(\mathbf{r})$ by multiplying with an additional measure factor $4\pi r^2$ in three dimensions, is compared with Monte-Carlo data for a WLC in Fig. 2 for several values of $\ell_p/L$.

### 2.1.4 WLC under a strong stretching force

We calculate the nonlinear response of the WBR to a strong stretching force $f$ acting at the ends. In the WBR parametrization, the Hamiltonian of a chain stretched by the force $f$ reads

$$\mathcal{H}_f = \mathcal{H}_{WLC} + \mathcal{H}_{ext} \approx \frac{\kappa}{2}\int_0^L \mathrm{ds}\left[\mathbf{r}_\perp''(s)\right]^2 + \frac{f}{2}\int_0^L \mathrm{ds}\left[\mathbf{r}_\perp'(s)\right]^2, \qquad (7)$$

where the last term $\mathcal{H}_{ext}$ is the work done by the external stretching force $f$, which is calculated from $\mathcal{H}_{ext} \equiv -\mathbf{f}\mathbf{R} = f\,r_\parallel(L) + const.$ using the approximate local arc-length constraint, Eq. (4). Since we are primarily interested in a qualitative discussion (rather than in numerically exact prefactors), we employ scaling arguments to find the asymptotic force-extension relation for the WLC. First we observe the occurrence of a characteristic length scale $\ell_f \equiv \sqrt{\kappa/f}$ of the force, which is obtained by equating the two contributions to the
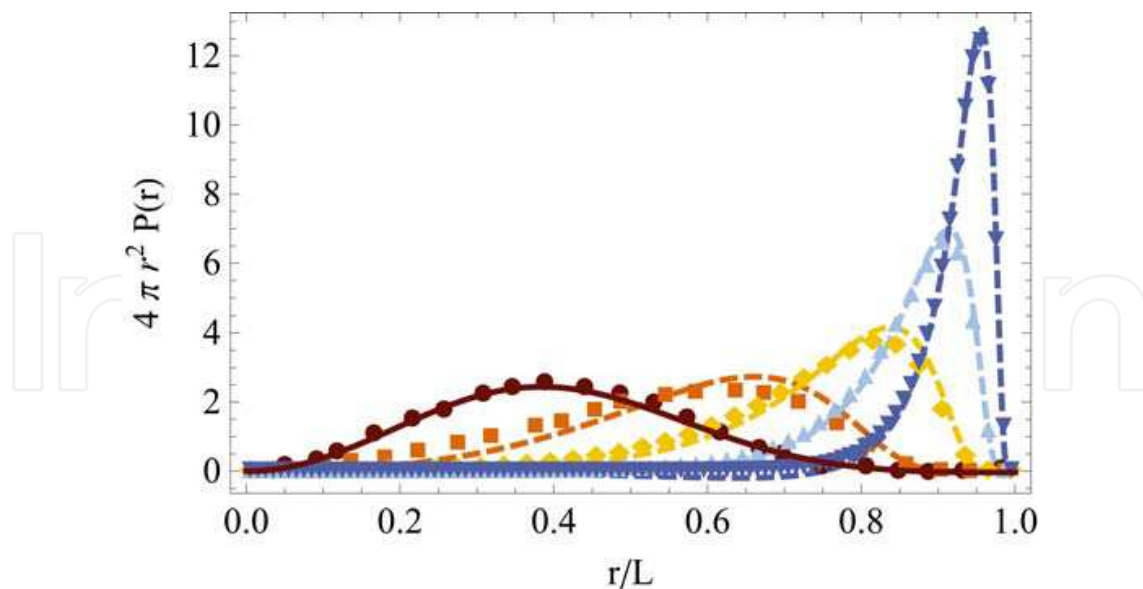
Fig. 2. Isotropic radial distribution function for a WLC of different $\ell_p/L$ = 0.1, 0.2, 0.5, 1, 2 from left to right. Shown is the asymptotic formula Eq. (6) (dashed lines) and the Daniels approximation (Daniels, 1950; Yamakawa, 1971) (solid line), compared with Monte Carlo simulation data (from Wilhelm & Frey (1996) for $\ell_p/L$ = 0.1, 0.2 and kindly provided by Sebastian Schöbl for $\ell_p/L$ = 0.5, 1, 2; symbols).

Hamiltonian, Eq. (7). It indicates the length of unperturbed chain sections with a stored length $r_\parallel(\ell_f) \simeq \ell_f^2 / \ell_p$. For strong stretching forces, the chain may thus be viewed as a taut string of a number $L/\ell_f$ of subsections of length $\ell_f$, and the asymptotic end-to-end distance follows as $R(f) = L - r_{\parallel,f}(L)$ from the total contraction $r_{\parallel,f}(L)$ of the chain,

$$ r_{\parallel,f}(L) \sim \frac{L r_\parallel(\ell_f)}{\ell_f} \simeq \frac{L \ell_f}{\ell_p} = L \sqrt{\frac{k_B T}{\ell_p f}}. \tag{8} $$

This estimate differs from the exact asymptotic result merely by a factor of 1/2 (Fixman & Kovac, 1973; Marko & Siggia, 1995).

## 2.2 Dynamics of the WBR
### 2.2.1 Equation of motion of the WBR and the fluctuation-dissipation theorem
We formulate the linearized Langevin equations of motion of an overdamped WLC in a viscous solvent. They derive from the WLC Hamiltonian, Eq. (1), and we note that the elastic force per unit length is given by $\mathbf{f}_{el} = -\delta \mathcal{H}/\delta \mathbf{r}$, where $\mathcal{H}$ is a sum of two contributions:

$$ \mathcal{H} = \mathcal{H}_{WLC} + \frac{1}{2} \int_0^L \mathrm{d}s\, f(s,t) \big[ \mathbf{r}'(s) \big]^2. $$

Here, a Lagrange multiplier force $f(s, t)$ enforces the local inextensibility constraint of the WLC, Eq. (2) (Goldstein & Langer, 1995). It has the physical interpretation of a local backbone tension. The friction force per unit length $\mathbf{f}_{visc} = -\zeta \dot{\mathbf{r}}$ is in the free-draining approximation mediated by a friction tensor

$$\boldsymbol{\zeta} \equiv [\zeta_\perp (1 - \mathbf{r}' \otimes \mathbf{r}') + \zeta_\parallel \mathbf{r}' \otimes \mathbf{r}'],$$

that reflects the anisotropic hydrodynamic interactions to leading order in two distinct friction coefficients $\zeta_\parallel$ and $\zeta_\perp$ for longitudinal and transverse motion, respectively (Doi & Edwards, 1988). To distinguish between contour length and time derivatives, we use primes and dots, respectively. Improved approximations for the viscous drag lead to logarithmic corrections to the linearized dynamics of a WBR (Granek, 1997; Glaser et al., 2008). The external and the stochastic thermal force per unit length are denoted by $\mathbf{g}$ and $\boldsymbol{\xi}$, respectively. Then, the linearized projected Langevin equations of motion follow from a balance of forces $\mathbf{f}_{visc} + \mathbf{f}_{el} + \mathbf{g} + \boldsymbol{\xi} = \mathbf{0}$ as

$$\zeta_\perp \dot{\mathbf{r}}_\perp = -\kappa \mathbf{r}_\perp''' + f\mathbf{r}_\perp'' + \mathbf{g}_\perp + \boldsymbol{\xi}_\perp,$$
$$f' = \mathbf{g}_\parallel. \tag{9}$$

In order to arrive at Eq. (9), we expanded the equations to linear order in $\mathbf{r}_\perp$ using Eq. (2) (Hallatschek et al., 2007a). We also approximated $f \approx const.$ in the WBR-limit. Its leading $(s, t)$-dependence is however accessible via a dedicated perturbation scheme (see Sec. 2.2.3 below). The equations are completed by the correlations of the Gaussian distributed stochastic force density $\boldsymbol{\xi}$,

$$\langle \xi_{\perp,i}(s,t) \rangle = 0,$$
$$\langle \xi_{\perp,i}(s,t)\xi_{\perp,j}(s',t') \rangle = 2k_B T \zeta_{\perp,ij}\delta(t-t')\delta(s-s').$$

These correlations are dictated by the fluctuation-dissipation theorem, which establishes a relation between the linear response of the chain $\langle \mathbf{r}(s, t) \rangle_{\mathbf{g}}$ and its equilibrium conformational correlations,

$$\frac{\delta \langle r_i(s,t) \rangle_{\mathbf{g}}}{\delta g_j(s',t')} = -\frac{\theta(t-t')}{k_B T}\frac{\mathrm{d}}{\mathrm{d}t}\langle r_i(s,t-t')r_j(s',0) \rangle \qquad \text{(FDT)}. \tag{10}$$

The FDT can be formulated for all systems in thermal equilibrium (Chaikin & Lubensky, 1995).

### 2.2.2 Linear response of a WBR to a transverse force

We employ scaling arguments again to find an approximate solution to Eq. (9) for the linear *dynamic* response of a WBR to a transverse step force $\mathbf{G}_\perp$, acting for times $t > 0$ at $s = s'$, i.e. $\mathbf{g}_\perp(s, t) = \mathbf{G}_\perp \delta(s - s')\theta(t)$ with $f = 0$. It causes a growing indentation of width $\ell_\perp(t)$ and depth $\langle \mathbf{r}_\perp(s', t) \rangle_{\mathbf{g}_\perp}$, both of which are to be determined. The width $\ell_\perp(t)$ is inferred from the thermally averaged Eq. (9), which reads $\zeta_\perp \mathbf{r}_\perp / t \simeq \kappa \mathbf{r}_\perp / \ell_\perp^4(t)$ on the scaling level for $s \neq s'$, yielding $\ell_\perp(t) \simeq (\kappa t/\zeta_\perp)^{1/4}$. To estimate $\langle \mathbf{r}_\perp \rangle_{\mathbf{g}_\perp}$, we carry out the ensemble average of Eq. (9) again and integrate over the spatial coordinate $s$, which gives:

$$\zeta_\perp \ell_\perp(t)\langle \dot{\mathbf{r}}_\perp \rangle_{\mathbf{g}_\perp} = \mathbf{G}_\perp, \tag{11}$$

The dynamics can therefore be understood in terms of a Stokes formula with a friction coefficient $\zeta_\perp(t) = \zeta_\perp \ell_\perp(t)$ that grows in time, corresponding to the increasing subsection of

length $\ell_\perp(t)$ of the chain that is set into motion by the force $\mathbf{G}_\perp$. Eq. (11) then implies for the linear response $\langle \mathbf{r}_\perp \rangle_{\mathbf{g}_\perp}$ to the external force

$$\langle \mathbf{r}_\perp \rangle_{\mathbf{g}_\perp} \sim \mathbf{G}_\perp \frac{t^{3/4}}{\zeta_\perp^{3/4} \kappa^{1/4}}.$$

The above assumption of a purely transverse friction implied by the linearized Eq. (9) ceases to hold when further growth of the transverse indentation $\langle \mathbf{r}_\perp \rangle_{\mathbf{g}_\perp}$ is hindered by the limited availability of stored length, i.e. if additional contour length needs to be pulled in against longitudinal friction from the tails of the WBR. Thus transverse motion couples to longitudinal motion via a growing tension $f$ and slows down at (sufficiently) long times (Obermayer & Hallatschek, 2007).

### 2.2.3 WBR under tension

The longitudinal dynamic response of a WBR to a stretching force $G_\parallel = f$ acting on the ends for $t > 0$ can analogously be inferred from scaling arguments. On the scaling level, the averaged Eq. (9) leads to $\zeta_\perp / t \simeq \kappa / \ell_\perp^4(t) + f / \ell_\perp^2(t)$, which implies $\ell_\perp(t) \simeq (\kappa t / \zeta_\perp)^{1/4}$ for $t \ll t_f \equiv \kappa \zeta_\perp / f^2$ and $\ell_\perp(t) \simeq (ft / \zeta_\perp)^{1/2}$ for $t \gg t_f$. The distinction between short and long times $t \lesssim t_f$ is equivalent to the one between weak and strong forces, $f \lesssim (\kappa \zeta_\perp / t)^{1/2}$. The former, linear response may be calculated from the corresponding longitudinal fluctuations using the FDT, Eq. (10). The result is that both quantities scale with time as $t^{3/4}$ (Granek, 1997; Everaers et al., 1999), similar to the transverse response (see Sec. 2.2.2). The long-time longitudinal response is estimated by observing that the chain consists of $L/\ell_\perp(t)$ subsections of length $\ell_\perp(t)$, which, by definition, have equilibrated at time $t$, i.e. they have been pulled essentially straight by the external force. The condition of straight subsegments implies that their elongation is equal to their initial equilibrium contraction $r_\parallel(\ell_\perp) \simeq \ell_\perp^2(t) / \ell_p$ (see Sec. 2.1.2), but with the opposite sign. The total change in end-to-end distance of the polymer follows as

$$\Delta R(t) \equiv r_\parallel(L, t = 0) - \mathbf{r}_\parallel(L, t) \sim \frac{L\ell_\perp(t)}{\ell_p} \simeq \frac{Lf^{1/2} t^{1/2}}{\zeta_\perp^{1/2} \ell_p}, \tag{12}$$

for $\ell_\perp(t) \ll L$. This quantity saturates at its equilibrium value $r_\parallel(L) - r_{\parallel,f}(L)$ (see Sec. 2.1.4) when $\ell_\perp(t) \simeq L$.

If longitudinal friction was generated along the whole filament length $L$, the corresponding drag force $\zeta_\parallel L \Delta \dot{R}$ would exceed the external driving force $f$ for times $t \lesssim t^\star \simeq \zeta_\parallel^2 L^4 / \zeta_\perp \ell_p^2 f$ (Seifert et al., 1996; Ajdari et al., 1997; Everaers et al., 1999). This apparent contradiction indicates the breakdown of Eq. (12) at short times. It is avoided by considering that longitudinal friction is only generated inside a boundary layer of width $\ell_\parallel(t)$ growing with time, where the polymer contour is set into longitudinal motion. For the longitudinal motion, the length $\ell_\parallel(t)$ thus plays a role analogous to $\ell_\perp(t)$ for the perpendicular motion. Accordingly, $\ell_\parallel(t)$ can be defined by postulating an effective longitudinal Stokes equation, analogous to Eq. 11 for the transverse motion,

$$\zeta_\parallel \ell_\parallel(t) \Delta \dot{R}(t) \simeq f, \tag{13}$$

with a longitudinal friction coefficient $\zeta_\parallel \ell_\parallel(t)$. Comparison of Eq. (13) with Eq. (12) after replacing $L$ by $\ell_\parallel(t)$ yields $\ell_\parallel(t) \simeq (ft\zeta_\perp)^{1/4}(\ell_p / \zeta_\parallel)^{1/2}$ for strong stretching forces (Seifert et al., 1996). The 'longitudinal equilibration length' is larger than the transverse one by a factor $\ell_\parallel / \ell_\perp \approx [\ell_p / \ell_\perp(t)]^{1/2} \gtrsim (\ell_p / L)^{1/2} \gg 1$ (for a sufficiently stiff polymer), and thus grows faster. Propagation of the tension $f(s, t)$ therefore only needs to be taken into account at short times for which $\ell_\parallel(t) \ll L$, i.e. when the tension has not yet equilibrated.

A systematic analysis of the phenomenon of tension propagation builds on this strong separation of length scales $\ell_\parallel(t) \gg \ell_\perp(t)$ (Hallatschek et al., 2005; 2007a;b). Via a (stochastic) multiple scale perturbation theory one can establish a coarse-grained deterministic theory for the polymer dynamics under strong tension. The spatially varying deterministic tension $f(s, t)$ is extracted by averaging over the transverse thermal fluctuations on short length scales. Previously known scaling results were recovered from this systematic theory as intermediate asymptotic regimes for specific scenarios, including pulling on the polymer, release of tension, and sudden temperature quench. The practically relevant case of pulling on a pre-stressed (Obermayer et al., 2007) or even pre-straightened (Obermayer et al., 2009) polymer, such as a polymer held in an optical trap, has been shown to lead to a wealth of new dynamic regimes and to depend sensitively on the initial conditions. Based on these results, the complex rheological modulus $G^\star(\omega) = G'(\omega) + iG''(\omega)$ for the response of a single WLC to an oscillatory longitudinal force could be calculated, and was shown to exhibit a $G^\star(\omega) \propto \omega^{7/8}$-regime for high frequencies (Hiraiwa & Ohta, 2008; 2009). Similar results were obtained for a chain with slightly extensible bonds (Obermayer & Frey, 2009). In affine shear flow, tension propagation can be neglected and the high-frequency modulus scales as $G^\star(\omega) \propto \omega^{3/4}$ (Gittes & MacKintosh, 1998; Morse, 1998c; Pasquali et al., 2001; Hiraiwa & Ohta, 2009).

# 3. Cells and gels

## 3.1 The bottom-up strategy and basic mechanics of the actin cytoskeleton

In this section, we review recent progress in the study of semiflexible polymer networks as simplified model systems for the actin cytoskeleton of the living cell (Kroy, 2006), focusing on their material properties (Kasza et al., 2007) and highlighting analogies (and differences) between both systems. We thus evaluate the usefulness of the bottom-up approach to cell mechanics by considering concrete examples of the linear and nonlinear rheology of cells and gels.

The mechanical properties of cells are considerably influenced by the cell cortex as a thin membrane-bound F-actin network capable of bearing substantial load (Stricker et al., 2010), although the contribution due to other intracellular compartments cannot be neglected (Hoffman & Crocker, 2009). A multitude of rheological techniques has been developed to characterize the response of the cell to mechanical perturbations (see Fig. 3). One may distinguish between passive and active techniques, which correspond to observing the the spontaneous motion of embedded tracer particles or to probing the deformation in response to an applied force, respectively. Only in equilibrium materials these methods yield the same results, whereas in the cell, this is in general not the case (see Sec. 3.5 below). The linear mechanical behavior of the cell, as characterized by the frequency-dependent complex shear modulus $G^\star(\omega)$, can be measured by passive methods under suitable conditions e.g. of ATP depletion (Bursac et al., 2005; Hoffman et al., 2006) or by active methods. It is intermediate between that of a solid and a liquid, and it is thus called viscoelastic.
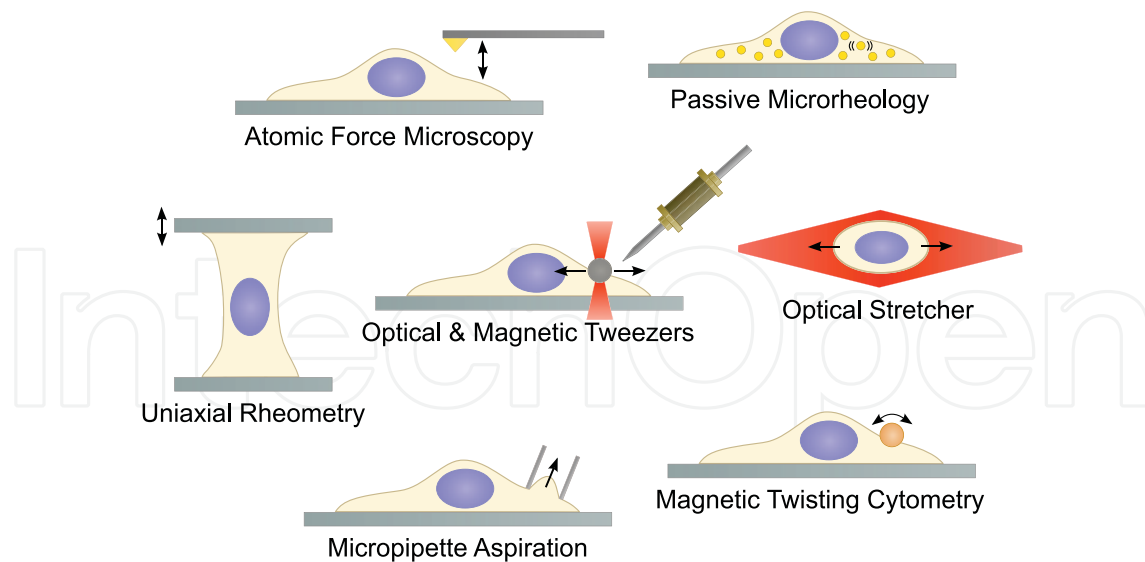
Fig. 3. Cells probed by common experimental methods, based on Kollmannsberger (2009) and Hoffman & Crocker (2009).

## 3.2 Importance of crosslinkers

The high-frequency shear-modulus of actin solutions and gels, a power-law resulting from single-filament dynamics (see Sec. 2.2.2 and Sections 4&5 below), crosses over to a rubber elastic plateau $G'(\omega) \sim G_0$ at low frequencies (Hinner et al., 1998; Gardel et al., 2004). This plateau is estimated by the tube model for entangled solutions (see Sec. 4 below) or the affine network model for gels (see Sec. 5 below). The difference between the absolute value of $G_0$ (on the order of $\approx$ 1Pa) and that of the weakly frequency-dependent shear modulus $G^\star(\omega)$ of cells (see Sec. 3.3 below; on the order of $\approx$ 1kPa) is now understood as a consequence of the different network elasticity in the absence or presence of crosslinkers and prestress. Networks of F-actin can be crosslinked using specific actin-binding-proteins (ABPs), and increasingly sophisticated studies have demonstrated that the relative crosslinker concentration, the type of crosslinker and even its molecular details provide fine-grained control over elastic and structural properties of the network (Gardel et al., 2004; 2006; Lieleg et al., 2010). Network elasticity is also determined by the flexibility of crosslinkers (Wagner et al., 2006). In addition, the network may be set under prestress, which can be externally applied (see Sec. 3.4 below) or internally generated, e.g. by molecular motors (see Sec. 3.5 below), which further increases the elasticity.

Cells choose between a multitude of different and partially redundant ABPs for crosslinking, but a large number of *in-vitro* studies concentrates on isolating the physical properties of networks crosslinked by a single type of molecule. This is justified by the fact that the rheological properties of composite networks containing different crosslinkers are largely determined by the crosslinker which outnumbers the other (Schmoller et al., 2008).

## 3.3 Plateau modulus vs. power-law rheology

The rheology of cells is well described by a power-law shear modulus $G^\star(\omega) \propto \omega^\beta$ at low frequencies with exponent $\beta = 0.1 - 0.25$, extending over up to three decades (Hoffman et al., 2006; Hoffman & Crocker, 2009). This has been interpreted as a sign of "glassy" dynamics (Fabry et al., 2001), as described by the generic model of "soft glassy rheology" (Sollich et al.,

1997). However, such slow dynamics was also recently observed in reconstituted biopolymer networks. High-precision dynamic light scattering studies have demonstrated that the plateau in the tracer particle MSD of actin solutions, which is related to the linear response function $G^*(\omega)$ via the FDT (see Sec. 2.2.1), is in reality slanted, corresponding to a dynamic structure factor $S(q, t)$ that exhibits slow logarithmic decay of density fluctuations over several decades in time (Semmrich et al., 2007). This has been parametrized with high precision by the "glassy wormlike chain" model (see Sec. 6 below). Experiments on filamin crosslinked networks, on the other hand, have shown that power-law rheology may readily arise in these systems (Gardel et al., 2006), where it might be due to the flexibility of crosslinkers (DiDonna & Levine, 2006). Given the variety of crosslinker types available to the cell, power-law rheology could also result from the superposition of different crosslinker binding/unbinding rates (Lieleg et al., 2008). Common to these explanations for the power-law rheology of cells is a broad distribution of length, time or energy scales, which is supposed to have its origin in the physics of the stiff polymers and their crosslinkers rather than in the genuinely biological cell dynamics. Therefore, its study should be possible not only *in-vivo*, but also in *in-vitro* reconstituted functional modules.

### 3.4 Nonlinear strain-softening and stiffening

However, the nonlinear rheology of cells differs from that of reconstituted gels at first sight. Cells have been reported to become stiffer *or* softer with increasing strain, depending on the applied deformation protocol, whereas reconstituted gels usually strain-stiffen. More specifically, cells under uniaxial loading displayed an elastic stiffening response (Fernández et al., 2006; Fernández & Ott, 2008), but when subjected to a transient stretch, the opposite response, i.e. fluidization and subsequent recovery emerged, as shown in Fig. 4, left (Trepat et al., 2007). The first response can be seen as analogous to observations of stiffening in actin gels (Gardel et al., 2004; 2006; Tharmann et al., 2007) or other biopolymer gels (Storm et al., 2005), for which it was explained by the affine network model (see Sec. 5 below), nonlinear crosslink flexibility (Broedersz et al., 2008) or network geometry (Onck et al., 2005). By contrast, the fluidization of cells and similar observations of viscoplasticity in the living cell (Fernández & Ott, 2008) have been suggested to arise from the breaking of cytoskeletal bonds (Trepat et al., 2007; Wolff et al., 2010) (see also Sec. 6 below).

A similar phenomenology has also been demonstrated for actin solutions undergoing a transition from strain softening to stiffening upon changing the solvent or ambient parameters or the deformation rate (Semmrich et al., 2007; 2008; Lieleg & Bausch, 2007) (Fig. 4, right). This behavior, resembling a glass transition, might arise due to weak sticky interactions between filaments. Thus, the coexistence of a fluidiziation and a reinforcement response in cells, analogous to the continuous transition from strain-softening to stiffening observed in actin gels, could be interpreted as a common feature of the material properties of both systems.

### 3.5 Towards active materials

The living cell operates far from thermodynamic equilibrium, and in the cytoskeleton, energy stored in the form of ATP is constantly transformed into mechanical energy e.g. through the activity of motor proteins such as myosin, or through the ATP-dependent polymerization of actin filaments. The cytoskeleton might therefore be characterized as an active material (Fletcher & Geissler, 2009). The effect of active processes on cell rheology is
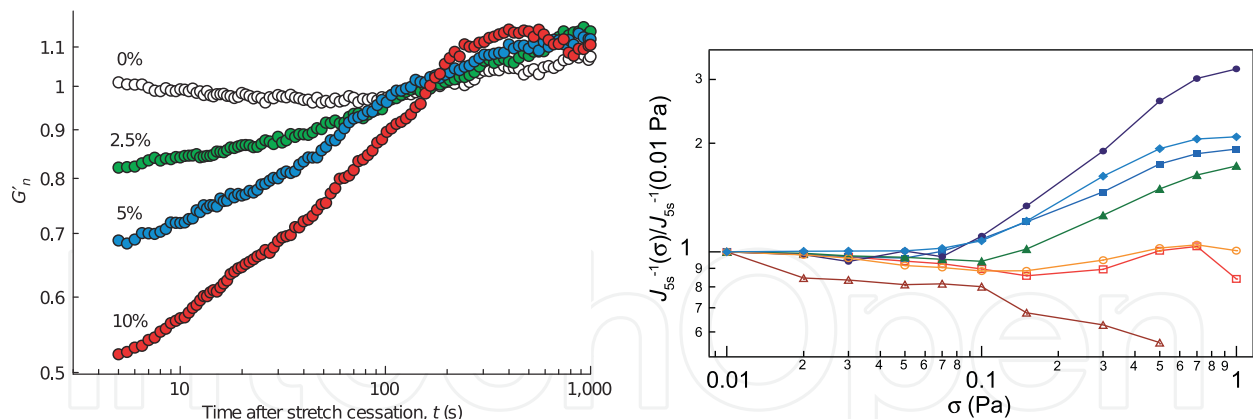
Fig. 4. *Left:* Fluidization and recovery of human airway smooth muscle cells after a single transient stretch, as measured by the normalized stiffness $G'_n$ for different stretch amplitudes. Adapted from Trepat et al. (2007). Copyright © 2007 by Macmillan Publishers Ltd. *Right:* Temperature-induced transition from strain softening to stiffening in entangled F-actin solutions. The inverse of the normalized creep compliance $J$ as a function of the applied stress $\sigma$ for various temperatures from $T = 27 − 18°C$ (bottom to top). Adapted from Semmrich et al. (2007). Copyright © 2007 by The National Academy of Sciences of the USA.

signalled by the breakdown of the fluctuation-dissipation theorem (FDT) (see Sec. 2.2.1) (Lau et al., 2003; Bursac et al., 2005). Thus, in contrast to equilibrium materials, the linear response function $G^{\star}(\omega)$ can not be inferred from looking at the spontaneous fluctuations, e.g. of the position of a probe particle embedded in the cell, and in the presence of non-equilibrium fluctuations, it can only be obtained by active measurements. On the other hand, by combining passive and active methods in the same experiment, non-equilibrium contributions to the spontaneous fluctuations can be measured. By this method, a breakdown of the FDT at frequencies below 10Hz due to active motor-induced forces has been demonstrated in actin-myosin gels (Mizuno et al., 2007) and similarly in cells (Mizuno et al., 2009). Active processes driven by molecular motors lead to a variety of new and interesting phenomena in reconstituted systems (MacKintosh & Schmidt, 2010), including fluidization of actin solutions (Humphrey et al., 2002), active fluctuations of stiff microtubules embedded in the actin cytoskeleton (Brangwynne et al., 2008), or stiffening of crosslinked gels due to contractile tension generated by motors (Mizuno et al., 2007; Koenderink et al., 2009). Since many cytoskeletal structures involve contractile elements, active reconstituted gels are highly relevant for a more complete understanding of cellular mechanics.

### 3.6 Conclusion

In conclusion, reconstituted cytoskeletal systems exhibit many of the salient features of cell mechanics and they seem ideally suited to further study the intriguing viscoelastic, non-linear and viscoplastic properties of the living cell. It has been suggested that cell mechanics may be understood in terms of a small number of "laws" (Trepat et al., 2008). Here we have presented evidence that biopolymer gels exhibit mechanical properties of comparable robustness and universality. Their structural basis consists of scaffolding fibers, such as F-actin, and these may be combined with a variety of crosslinkers and ultimately with active components. This demonstrates that using simple, polymer-based model systems it is possible to explain a large number of cell mechanical observations by minimal assumptions.

Theoretical descriptions are therefore useful to establish the link between the rheological properties at a higher level to the underlying microscopic structures.

## 4. Tube model

In this section, we address theories for entangled solutions of stiff polymers (see Sec. 3). In the absence of crosslinkers, their equilibrium properties are successfully and quantitatively described by models of topological interactions. Macroscopic resistance against shear arises from the mutual impenetrability of the polymers – to deform a test filament, surrounding filaments need to be pushed out of the way, as familiar from knotted strings. The mathematical problem posed by highly entangled solutions is sufficiently complicated that it eludes a rigorous solution (Edwards, 1967; Everaers et al., 2004), yet, the tube model provides a simple and successful phenomenological description of their macroscopic properties.

### 4.1 Tube model for flexible polymers

The tube model was introduced by S. F. Edwards for melts and solutions of flexible polymers (Edwards, 1967; Doi & Edwards, 1988). The idea is to circumvent the explicit discussion of the complicated topological constraints and to represent them, effectively, by a harmonic potential for a test polymer, which is thus confined to a narrow tube-like cage. The polymer may escape its cage very slowly by a snake-like diffusive motion called reptation (de Gennes, 1971; Doi & Edwards, 1988; Schweizer et al., 1997). Another mechanism consists in the sudden release of constraints, when the ends of confining polymers slide past the test polymer. The reptation time $\tau_d$ is very sensitive on the contour length $L$. From the longitudinal diffusion coefficient $D_\parallel \propto L^{-1}$ one estimates it as $\tau_d \simeq L^2/D_\parallel \propto L^3$ for large $L$ (de Gennes, 1971).

### 4.2 Tube model for semiflexible polymers

The principle of the tube model also applies to semiflexible polymers, with the main difference being the presence of an additional scale, the persistence length $\ell_p$. It gives rise to a tightly entangled regime (Morse, 1998a; Uchida et al., 2008), where $\ell_p$ is larger than the mesh size $\xi$ defined as $\xi \equiv \rho^{-1/2}$. Here, $\rho \equiv c_p L$ denotes the line concentration and $c_p$ the polymer concentration. In a tightly entangled solution, the transverse bending undulations of all polymers are confined. The typical time scale $\tau_e$ on which they equilibrate and thus constitute the tube is on the order of milliseconds in actin solutions (Semmrich et al., 2007). On the other hand, typical semiflexible actin filaments have tube renewal times $\tau_d$ on the order of hours (Käs et al., 1994; He et al., 2007). Thus $\tau_d$ is much longer than the time needed by the transverse bending undulations to explore the cage and one can treat the polymer solution as an effective equilibrium system with a quenched network topology on intermediate time scales $\tau_e \ll t \ll \tau_d$.

The success of the tube model relies on the fact that it requires only a small set of parameters to predict most properties of the rheology and the dynamics quantitatively. These parameters can be inferred from an analysis of the topological problem in simulations (Everaers et al., 2004) or from simple self-consistent scaling arguments. More specifically, the tightly entangled state of semiflexible polymer solutions is characterized by the mean-field tube radius $R$ and entanglement length $L_e \simeq R^{2/3}\ell_p^{1/3}$ of a test polymer, referring to the

magnitude of the confined transverse undulations of a WLC (see Eq. (5)) and the contour length between collisions, respectively (see Fig. 5, left) (Odijk, 1983; Semenov, 1986). The dependence of the values of $R$ and $L_e$ on monomer concentration $c \propto \rho$ is readily estimated by considering the binary collision of a test polymer with an obstacle filament. The average number of collisions per entanglement segment is on the order of one, which gives $c_p L L_e R \simeq 1$. Defining $L_e$ as above, one then self-consistently obtains the tube radius $R \simeq \rho^{-3/5} \ell_p^{-1/5}$ and the entanglement length $L_e \simeq \rho^{-2/5} \ell_p^{1/5}$ (Semenov, 1986).

Macroscopic properties such as the plateau shear modulus $G_0$ or the osmotic compression modulus $\Pi(\rho)$ are expressed in terms of these fundamental parameters, and from the latter they inherit their characteristic concentration-dependence. Assuming that each collision of the test polymer with its tube contributes a free energy $k_B T$, the confinement free energy per filament scales as (Odijk, 1983; Isambert & Maggs, 1996; Burkhardt, 1995)

$$F \simeq \frac{k_B T L}{L_e} \sim \rho^{2/5}.$$

From this, the plateau shear modulus and the osmotic compression modulus are estimated as $G_0(\rho) \simeq \Pi(\rho) \equiv -N \partial F / \partial V \simeq k_B T \rho / L_e \propto c^{7/5}$ (Isambert & Maggs (1996); Morse (1998b)). This characteristic dependence on concentration has indeed been observed experimentally (Hinner et al., 1998; Tassieri et al., 2008; Vincent et al., 2007).

The tube model predicts a high-frequency limiting form of the complex, frequency-dependent shear modulus, resulting from the dynamic response of longitudinal fluctuations (see Sec. 2.2.3) (Morse, 1998c; Gittes & MacKintosh, 1998),

$$G^{\star}(\omega) = \frac{1}{15} \kappa \rho \ell_p (-2i\zeta / \kappa)^{3/4} \omega^{3/4}. \tag{14}$$

This high-frequency modulus has been confirmed experimentally (Gittes et al., 1997; Gisler & Weitz, 1999; Koenderink et al., 2006).

### 4.2.1 Microscopic models for the tube

The intuition associated with the tube model has been confirmed in single-molecule experiments. Because of the relatively larger dimensions of F-actin compared to flexible polymers, the tube around a single actin filament in entangled solution can directly be visualized microscopically using fluorescence labeling techniques (Käs et al., 1994). The possibility to measure the tube radius directly has spurred the development of quantitative tube models, based on a self-consistent binary collision approximation (BCA) (Morse, 2001; Hinsch et al., 2007) and an effective medium approximation (EMA) (Morse, 2001). These models predict the value of the tube radius relying on an analysis of the entanglement topology. For example, the BCA considers pairwise collisions of two weakly bending rods in a simple binary topology – "above" or "below". In a self-consistent calculation, the tube's strength is calculated as the cumulative effect of pair collisions in all possible configurations. The EMA, on the other hand, only discusses the average effect of the topological interactions. In this approximation, the polymer is coupled to an effective elastic background medium. Both theories give rise to conflicting predictions for the concentration-dependence of $R$ and $L_e$, opening a debate on the appropriate theoretical description of semiflexible polymer solutions, and they have therefore been challenged by experiments
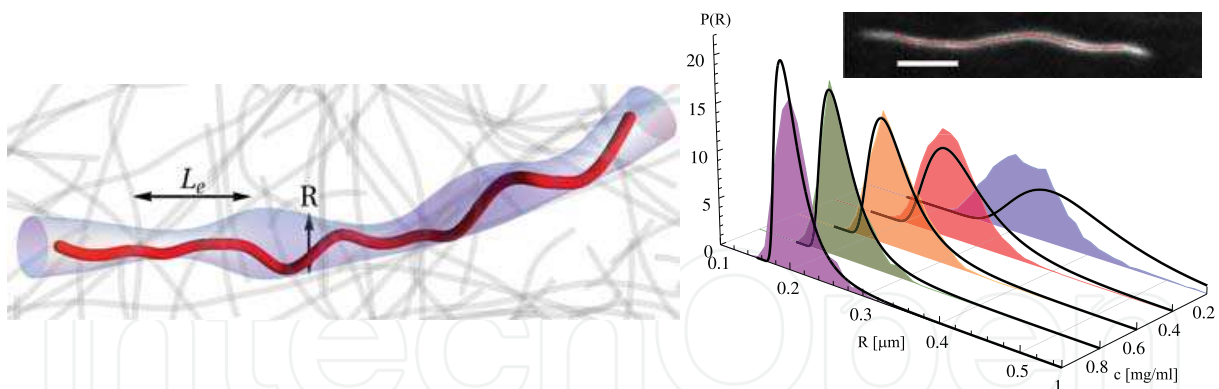
Fig. 5. *Left:* A stiff polymer confined in a tube of spatially varying radius $R$; $L_e$: entanglement length. Background polymers are depicted in gray. *Right:* Tube radius distribution $P(R)$ measured in entangled solutions of F-actin at different concentrations (shaded areas). Solid lines represent a global fit by a segment fluid theory. *Inset*: Superimposed confocal microscopy images of a fluorescent actin filament in a background solution and a spline representing the tube backbone; scale bar: 5µm. The width of the tube is inferred from Gaussian fits to the transverse intensity profile. From Glaser et al. (2010). Copyright © 2010 by The American Physical Society.

and simulations, which have either been in favor of the BCA (Romanowska et al., 2009; Wang et al., 2010; Ramanathan & Morse, 2007) or of the EMA (Tassieri et al., 2008). This controversy results in part from the close match of the scaling exponents in the BCA ($R \propto c^{-3/5}$) and the EMA ($R \propto c^{-1/2}$), suggesting that an unambiguous distinction between the two power-laws is extremely difficult to establish experimentally (Tassieri et al., 2008). In addition, respective conclusions must be drawn with care, since experiments typically yield skewed distributions of the tube radius, rendering an interpretation in terms of mere average values problematic (Wang et al., 2010; Glaser et al., 2010).

### 4.2.2 Tube width fluctuations

Indeed, experiments (Käs et al., 1994; Dichtl & Sackmann, 1999; Romanowska et al., 2009; Wang et al., 2010) and simulations (Hinsch et al., 2007) indicated that the assumption of a uniform tube width is a severe approximation. Pronounced tube fluctuations along a single actin filament have been measured by fluorescence microscopy (Glaser et al., 2010), as sketched in Fig. 5, left, and they can be analyzed by a systematic BCA-based theory. This theory extends D. Morse's mean-field approach and allows for a comprehensive characterization of the microstructure of entangled solutions. It predicts a tube radius distribution $P(R)$ quantifying the observed heterogeneities and compares favorably with experiments (see Fig. 5, right). An analysis of small remaining discrepancies in this comparison attributes them to collective modes of the effective medium. This suggests a way how to combine the BCA and the EMA to achieve a practically perfect explanation of the experimental data in the future (Glaser, 2010).

### 4.3 Recent developments and open problems

We now discuss experimental findings which, at first sight, seem to contradict the predictions of the tube model. For example, in experiments, the curvature distribution of the tube's primitive path has been measured and large curvatures occurred with a higher

frequency than expected for a free polymer (Romanowska et al., 2009). This was corroborated by computer simulations, where the same effect has been shown to occur when filament ends were allowed to move freely and to slide past fixed obstacles (Hinsch & Frey, 2009), suggesting that one may interpret it as a consequence of finite filament length.

A further observation is the slow logarithmic increase of the tube radius with time (see Sec. 3.3 and Sec. 6 below), which leads to an effective "softening" of the tube. In practice, however, this time dependence is weak, and, depending on the application, it may be accounted for by measuring an effectively saturated value of the tube radius.

Finally, let us comment on the nonlinear rheology. The response of physically entangled solutions to nonlinear strains is predicted by a nonlinear tube model, in which the tube is allowed to compress or expand (Morse, 1999; Fernández et al., 2009). The predicted universal strain-softening response is in contrast with the gradual transition from softening to stiffening in actin solutions (see Sec. 3.4 and Fig. 4, right), which has been interpreted as a consequence of weak crosslinking. On the other hand, the parameter changes that controlled this transition had little or no effect on the linear shear modulus (Semmrich et al., 2007; 2008). One might interpret this and the results of this section in the sense that the tube model has been validated for the linear response regime, while its predictions are overshadowed by (spurious) adhesion and crosslinking effects in most non-linear measurements at finite shear rates.

In summary, the tube model provides a detailed quantitative explanation of the mechanical properties of entangled polymer solutions. It reveals the important role of topological interactions in simple reconstituted cytoskeletal systems and serves as a well-defined reference description for studies of nontrivial dynamic and nonlinear effects. In a further step towards complexity, crosslinkers may be added.

## 5. Affine network model

The phenomenology of cytoskeletal networks with crosslinkers is broad and depends on a multitude of parameters, such as crosslinker type (rigid or flexible), crosslinker time scale (on/off-rate) and crosslinker/filament ratio (weakly or strongly crosslinked). After discussing elementary affine and non-affine deformation mechanisms, we give an outline of the affine network model as a simple zeroth order explanation for many of the observed effects in crosslinked networks, and we review progress on their understanding beyond the simplifying assumption of affine deformations.

Crosslinkers mediate local interactions between polymers. For the protein filament meshworks that make up the cytoskeleton, their action relies on specific binding sites on the polymers, in other words, they induce short-ranged, "patchy" attractions. In cases of extremely long bond lifetimes, these attractions may be modeled as geometric constraints (in addition to the above mentioned topological constraints due to the impenetrability of the polymer backbones). One commonly accounts for the presence of crosslinkers by introducing a new characteristic length scale $L_c$, representative of the mean distance between crosslinking sites along a single filament (MacKintosh, 2006), which is distinct from the entanglement length $L_e$ and the geometrical mesh size $\xi$. On the level of a single filament, two different modes of deformation exist: longitudinal stretching/compression and transverse bending. Since, for rod-like networks, simple shear amounts to rotation and stretching/compression of filaments, only these latter modes should be relevant in a purely affine deformation. On the other hand, cooperative deformation mechanisms may result in

non-affine deformations involving bending of filaments. If the response to shear was dominated by non-affine filament bending, the plateau modulus of a densely crosslinked network approximated as a simple cubic mesh of semiflexible filaments with $\xi \simeq L_c$ would be expected to scale as (Kroy & Frey, 1996)

$$G_0 \simeq \frac{k_B T \ell_p}{\xi^4} \propto k_B T \ell_p c^2. \tag{15}$$

In the case of purely affine stretching, the modulus of the network originates from the mechanical response of a single WLC of length $L_c$. Stretching it an amount $\delta \ell \equiv \gamma L_c$ in the linear regime requires a force $f \simeq k_B T \ell_p^2 \delta \ell / L_c^4$ (MacKintosh et al., 1995). Defining the stress as $\sigma = f / \xi^2$, the shear modulus follows as

$$G_0 \equiv \frac{\sigma}{\gamma} \simeq \frac{k_B T \ell_p^2}{L_c^3 \xi^2}. \tag{15}$$

This is the rubber elasticity modulus of the affine semiflexible network model, which depends on filament and crosslinker concentration via the mesh size $\xi$ and the cross-linker distance $L_c$. Using a plausible (ad-hoc) parametrization of the latter, agreement between Eq. (15) and experimental data for actin (Gardel et al., 2004; Tharmann et al., 2007) and intermediate filament networks (Lin et al., 2010) can be obtained.

The corresponding high-frequency modulus $G^{\star}(\omega)$ may be estimated from the rubber elastic modulus Eq. (15) in close analogy to the single-polymer results of Sec. 2.2.3, by replacing $L_c$ with the dynamic equilibration length $\ell_\perp(t)$ for weak forces, evaluated at $t = i\omega$, yielding $G^{\star}(\omega) \simeq k_B T \ell_p^2 / \xi^2 \ell_\perp^3 (t = i\omega) \propto \omega^{3/4}$. The exact asymptotic form of this complex viscoelastic high-frequency modulus is again given by Eq. (14), which includes prefactors and which constitutes a universal asymptotic result independent of the crosslinker or affinity length scale $L_c$. It has been verified for crosslinked networks and entangled solutions of F-actin (Koenderink et al., 2006).

The affine network model provides a simple natural explanation for the observed strain stiffening response observed for *in-vitro* networks and cells (see Sec.3.4) in terms of the nonlinear force-extension relation of a single WLC (see Sec. 2.1.4). Since it follows from Eq. (8) that $f \propto [L - R(f)]^{-2}$, the nonlinear differential modulus is thus obtained as (see Sec. 2.1.4) (MacKintosh et al., 1995; MacKintosh, 2006)

$$K' \equiv \frac{d\sigma}{d\gamma} \propto \frac{df}{dR} \propto f^{3/2} \propto \sigma^{3/2}. \tag{16}$$

Let us now turn to the question under which conditions the affine or non-affine deformation mechanisms prevail. This problem has been studied by simulations of two-dimensional crosslinked random fiber networks in the mechanical limit (Wilhelm & Frey, 2003; Head et al., 2003), and it was found that the transition from the non-affine bending to the affine stretching regime occurs for high crosslink densities and/or long fibers. The afine to non-affine transition of mechanical fibers has also been observed in regular networks based on a triangular geometry (Das et al., 2007). Strain field visualization in F-actin networks indeed seems to provide some evidence for a cross-over between distinct deformation modes,

depending on the ratio of polymer length to a characteristic non-affinity length scale (Liu et al., 2007). Heussinger and Frey have however shown by taking into account thermal fluctuations that affine deformations are unstable and non-affine intermediate asymptotic scaling regimes of the shear modulus dominate the mechanical response instead (Heussinger & Frey, 2006a;b). These are characterized by filament-filament correlations, which are not taken into account in the affine network model. Further simulation studies show that the strain field is in general non-affine (Onck et al., 2005), and that homogeneously crosslinked networks are softer in the linear regime and stiffen at higher strains than predicted by the affine network model (Huisman et al., 2008).

Moreover, the stiffening exponent of Eq. (16) is not universal (see also Sec. 3.4), as for example in filamin-crosslinked networks, strain-stiffening with an exponent close to one is observed (Gardel et al., 2006). Thus, models for flexible crosslinkers such as filamin have also been discussed. These may either be represented as a series of domains capable of unfolding (DiDonna & Levine, 2006), or as inextensible wormlike chains (Broedersz et al., 2008), leading to a softening or stiffening response, respectively. Recently theoretically studied problems also include thermodynamic properties and complex phase diagrams of polymer networks (Borukhov et al., 2005; Benetatos & Zippelius, 2007). An interesting interplay between single polymer and crosslinker dynamics arises in transiently connected networks, where the kinetics of the crosslinker leads to an additional viscous dissipation mechanism (Lieleg et al., 2008; Wolff et al., 2010) (see Sec. 6 below).

## 6. Towards viscoelastic and inelastic dynamics - the glassy wormlike chain

A study of semiflexible polymer dynamics in purely entangled solutions revealed that instead of a strict tube constraint, an additional relaxation mechanism exists at long times. More specifically, simulations have shown that the tube potential softens with time (Zhou & Larson, 2006; Ramanathan & Morse, 2007), implying a time-dependent tube radius. Analogous observations in flexible polymer melts have been attributed to constraint release (Vaca Chávez & Saalwächter, 2010). The dynamic structure factor of entangled F-actin solutions exhibited slow logarithmic decay beyond the cross-over time from free to confined polymer modes, extending over five decades in time (see Fig. 6, right, black curves) (Semmrich et al., 2007). The glassy wormlike chain (GWLC) model interprets this by an exponentially stretched relaxation time spectrum of the normal modes of an ordinary WLC on time scales longer than the equilibration time $\tau_\Lambda \simeq \tau_e$ (Kroy & Glaser, 2007; Kroy, 2008). This is accomplished by prescribing a modified relaxation time $\tau_\lambda$ for collective excitations of wavelength $\lambda$ by

$$\tau_\lambda \to \tilde{\tau}_\lambda = \begin{cases} \tau_\lambda, & \lambda < \Lambda \\ \tau_\lambda \exp[\varepsilon(\lambda/\Lambda - 1)], & \lambda > \Lambda. \end{cases}$$

All relaxation times of bending modes of a wavelength longer than the characteristic interaction or bond length $\Lambda$ – which may be different from the entanglement length (Glaser et al., 2008) – are thus multiplied by an Arrhenius factor involving the energy $\mathcal{E}k_BT$, and the number $\lambda/\Lambda - 1$ of interactions. The Arrhenius factors have been attributed to free energy barriers arising either from finite free energy costs for tube deformations or from sticky interactions. Using this prescription in explicit expressions for the dynamic structure factor
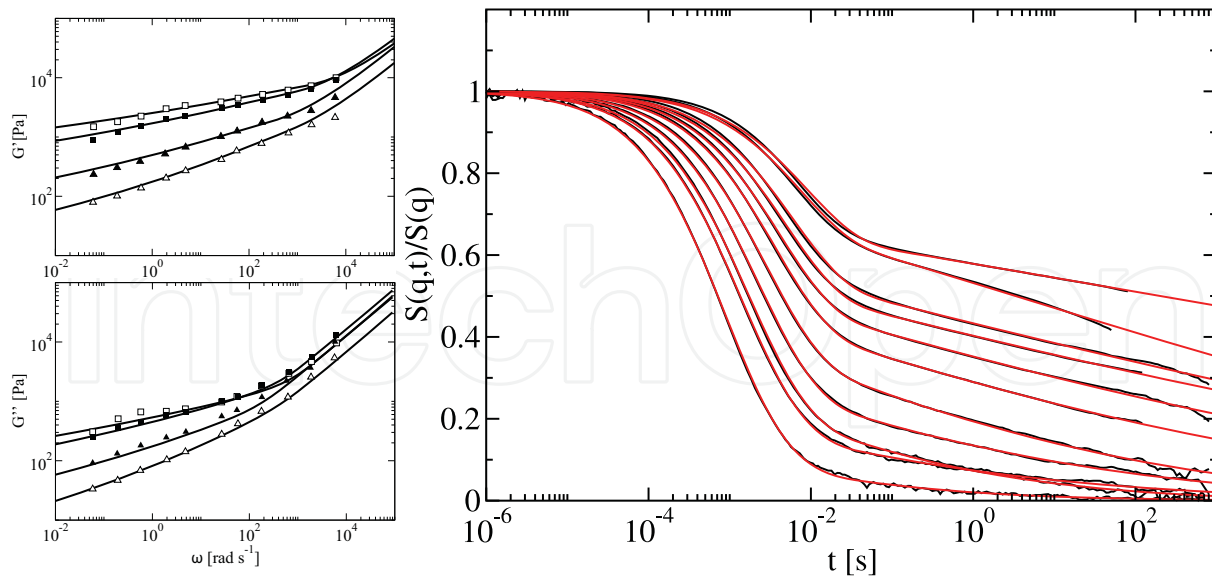
Fig. 6. *Left:* Storage and loss modulus $G'(\omega)$ and $G''(\omega)$ of human airway smooth muscle cells (symbols), for different pharmacological treatments. Solid lines are fits to the GWLC model described in Sec. 6. From Kroy & Glaser (2009). Copyright © 2009 by American Institute of Physics. Experimental data from Fabry et al. (2001). *Right*: Dynamic structure factor $S(q, t)$ of entangled F-actin solutions at various wave vectors $q$ (black curves) fitted by the GWLC model (red curves) proposed in Sec. 6. Adapted from Semmrich et al. (2007). Copyright © 2007 by The National Academy of Sciences of the USA.

of stiff polymer solutions (Kroy & Frey, 1997; Glaser et al., 2008) yields excellent agreement of the model predictions with the data (Fig. 6, right, red curves). The "macrorheological modulus" $G^\star(\omega)$ of a GWLC is obtained by combining the affine network model of Sec. 5 with the stretched relaxation times of the GWLC. It exhibits (near) power-law rheology, in very good agreement with rheological data on live cells, see Fig. 6, left (Kroy & Glaser, 2009). Concerning the nonlinear response, the model accounts for the mutually opposite influences of stiffening due to backbone tension and the lowering of the energy barrier height $\mathcal{E}$ under the influence of an external force. Hence, the nonlinear differential shear modulus of a GWLC shows a variable degree of stiffening depending on the value of $\mathcal{E}$, followed by a softening response at high strains, which is in qualitative agreement with the experimental observations shown in Fig. 4, right.

The GWLC thus provides an efficient phenomenological description of slow dynamics in entangled solutions of stiff polymers, and conceptually, it might also be applied to weakly crosslinked networks. Indeed, the model has recently been extended to account for bond kinetics with defined rates and under the influence of a force (Wolff et al., 2010). The corresponding model for inelastic deformations in sticky polymer solutions evaluates the macroscopic shear modulus of the GWLC using a dynamic inter-bond distance $\Lambda(t)$ that accounts for the slow inelastic network evolution. In this scheme, it is straightforward to include the effect of prestress or backbone tension. It is then possible to account for the experimentally observed fluidiziation and recovery of live cells after transient shear deformations (see Fig. 4, left).

## 7. Summary and conclusion

The study of single biopolymers provides the basic knowledge necessary to describe their complex collective effects in a "bottom-up approach". The starting point of a description of stiff polymers is the wormlike chain model for a single semiflexible polymer, which already exhibits a rich phenomenology. Entangled solutions of stiff polymers are appropriately described by the tube model. In particular, we discussed heterogeneities of the tube width. The affine network model provides a simple explanation for the mechanics of densely crosslinked networks. Models of the viscoelastic and inelastic response of weakly and transiently crosslinked networks substantially extend prevailing theoretical approaches for cytoskeletal networks. Clearly, the development of mathematical toy models and systematic theories will remain a crucial element in the approach to a microscopic understanding of the origins of the remarkable mechanical properties of living matter.

## 8. Acknowledgments

## 9. References

Ajdari, A., Jülicher, F. & Maggs, A. (1997). Pulling on a Filament, *J. Phys. (France)* 7(7): 823–826.

Alim, K. & Frey, E. (2007). Shapes of Semiflexible Polymer Rings, *Phys. Rev. Lett.* 99(19): 198102.

Baczynski, K., Lipowsky, R. & Kierfeld, J. (2007). Stretching of buckled filaments by thermal fluctuations, *Phys. Rev. E: Stat., Nonlinear, Soft Matter Phys.* 76(6): 061914.

Bao, G. & Suresh, S. (2003). Cell and molecular mechanics of biological materials, *Nat. Mater.* 2(11): 715–25.

Bausch, A. & Kroy, K. (2006). A bottom-up approach to cell mechanics, *Nat. Phys.* 2(4): 231–238.

Benetatos, P. & Zippelius, A. (2007). Anisotropic Random Networks of Semiflexible Polymers, *Phys. Rev. Lett.* 99(19): 198301.

Borukhov, I., Bruinsma, R. F., Gelbart, W. M. & Liu, A. J. (2005). Structural polymorphism of the cytoskeleton: a model of linker-assisted filament aggregation., *Proc. Natl. Acad. Sci. U. S. A.* 102(10): 3673–8.

Brangwynne, C., Koenderink, G., MacKintosh, F. & Weitz, D. (2008). Nonequilibrium Microtubule Fluctuations in a Model Cytoskeleton, *Phys. Rev. Lett.* 100(11): 118104.

Brangwynne, C. P., MacKintosh, F. C., Kumar, S., Geisse, N. A., Talbot, J., Mahadevan, L., Parker, K. K., Ingber, D. E. & Weitz, D. A. (2006). Microtubules can bear enhanced compressive loads in living cells because of lateral reinforcement, *J. Cell. Biol.* 173(5): 733–41.

Broedersz, C., Storm, C. & MacKintosh, F. (2008). Nonlinear Elasticity of Composite Networks of Stiff Biopolymers with Flexible Linkers, *Phys. Rev. Lett.* 101(11): 118103.

Burkhardt, T. (1995). Free energy of a semiflexible polymer confined along an axis, *J. Phys. A.: Math. Gen.* 28: L629–635.

Bursac, P., Lenormand, G., Fabry, B., Oliver, M., Weitz, D. A., Viasnoff, V., Butler, J. P. & Fredberg, J. J. (2005). Cytoskeletal remodelling and slow dynamics in the living cell, *Nat. Mater.* 4(7): 557–61.

Bustamante, C., Bryant, Z. & Smith, S. (2003). Ten years of tension: single-molecule DNA mechanics, *Nature* 421(6921): 423–427.

Bustamante, C., Marko, J., Siggia, E. & Smith, S. (1994). Entropic Elasticity of lambda-Phage DNA, *Science* 265(5178): 1599–1600.

Caliskan, G., Hyeon, C., Perez-Salas, U., Briber, R., Woodson, S. & Thirumalai, D. (2005). Persistence Length Changes Dramatically as RNA Folds, *Phys. Rev. Lett.* 95(26): 268303.

Chaikin, P. & Lubensky, T. (1995). *Principles of condensed matter physics*, Cambridge University Press, Cambridge.

Daniels, H. (1950). The statistical theory of stiff chains, *Proc. Roy. Soc. Edinburgh* 63: 290–311.

Das, M., MacKintosh, F. & Levine, A. (2007). Effective Medium Theory of Semiflexible Filamentous Networks, *Phys. Rev. Lett.* 99(3): 038101.

de Gennes, P. G. (1971). Reptation of a Polymer Chain in the Presence of Fixed Obstacles, *J. Chem. Phys.* 55(2): 572-579.

Dichtl, M. & Sackmann, E. (1999). Colloidal probe study of short time local and long time reptational motion of semiflexible macromolecules in entangled networks, *New J. Phys.* 1: 18.

DiDonna, B. & Levine, A. (2006). Filamin Cross-Linked Semiflexible Networks: Fragility under Strain, *Phys. Rev. Lett.* 97(6): 068104.

Discher, D., Dong, C., Fredberg, J. J., Guilak, F., Ingber, D., Janmey, P., Kamm, R. D., Schmid-Schönbein, G. W. & Weinbaum, S. (2009). Biomechanics: cell research and applications for the next decade, *Ann. Biomed. Eng.* 37(5): 847–59.

Doi, M. & Edwards, S. F. (1988). *The Theory of Polymer Dynamics*, Oxford University Press, Oxford.

Edwards, S. F. (1967). The statistical mechanics of polymerized material, *Proc. Phys. Soc. London* 92(1): 9–16.

Emanuel, M., Mohrbach, H., Sayar, M., Schiessel, H. & Kulić, I. (2007). Buckling of stiff polymers: Influence of thermal fluctuations, *Phys. Rev. E: Stat., Nonlinear, Soft Matter Phys.* 76(6): 061907.

Everaers, R., Jülicher, F., Ajdari, A. & Maggs, A. (1999). Dynamic Fluctuations of Semiflexible Filaments, *Phys. Rev. Lett.* 82(18): 3717–3720.

Everaers, R., Sukumaran, S. K., Grest, G. S., Svaneborg, C., Sivasubramanian, A. & Kremer, K. (2004). Rheology and microscopic topology of entangled polymeric liquids, *Science* 303(5659): 823–6.

Fabry, B., Maksym, G., Butler, J., Glogauer, M., Navajas, D. & Fredberg, J. (2001). Scaling the Microrheology of Living Cells, *Phys. Rev. Lett.* 87(14): 148102.

Farge, E. & Maggs, A. C. (1993). Dynamic scattering from semiflexible polymers, *Macromolecules* 26(19): 5041–5044.

Fernández, P., Grosser, S. & Kroy, K. (2009). A unit-cell approach to the nonlinear rheology of biopolymer solutions, *Soft Matter* 5(10): 2047-2056.

Fernández, P. & Ott, A. (2008). Single Cell Mechanics: Stress Stiffening and Kinematic Hardening, *Phys. Rev. Lett.* 100(23): 238102.

Fernández, P., Pullarkat, P. A. & Ott, A. (2006). A master relation defines the nonlinear viscoelasticity of single fibroblasts, *Biophys. J.* 90(10): 3796–805.

Fixman, M. & Kovac, J. (1973). *Polymer conformational statistics: III. Modified Gaussian models of stiff chains, J. Chem. Phys.* 58 (4):1564-1568.

Fletcher, D. A. & Geissler, P. L. (2009). Active biological materials, *Annu. Rev. Phys. Chem.* 60: 469–86.

Fletcher, D. A. & Mullins, R. D. (2010). Cell mechanics and the cytoskeleton, *Nature* 463(7280): 485–92.

Gardel, M. L., Nakamura, F., Hartwig, J. H., Crocker, J. C., Stossel, T. P. & Weitz, D. a. (2006). Prestressed F-actin networks cross-linked by hinged filamins replicate mechanical properties of cells., *Proc. Natl. Acad. Sci. U. S. A.* 103(6): 1762–7.

Gardel, M. L., Shin, J. H., MacKintosh, F. C., Mahadevan, L., Matsudaira, P. & Weitz, D. A. (2004). Elastic behavior of cross-linked and bundled actin networks, *Science* 304(5675): 1301–5.

Gisler, T. & Weitz, D. (1999). Scaling of the Microrheology of Semidilute F-Actin Solutions, *Phys. Rev. Lett.* 82(7): 1606–1609.

Gittes, F. & MacKintosh, F. (1998). Dynamic shear modulus of a semiflexible polymer network, *Phys. Rev. E: Stat., Nonlinear, Soft Matter Phys.* 58(2): R1241–R1244.

Gittes, F., Schnurr, B., Olmsted, P., MacKintosh, F. & Schmidt, C. (1997). Microscopic Viscoelasticity: Shear Moduli of Soft Materials Determined from Thermal Fluctuations, *Phys. Rev. Lett.* 79(17): 3286–3289.

Glaser, J. (2010). Unpublished.

Glaser, J., Chakraborty, D., Kroy, K., Lauter, I., Degawa, M., Kirchgeßner, N., Hoffmann, B., Merkel, R. & Giesen, M. (2010). Tube Width Fluctuations in F-Actin Solutions, *Phys. Rev. Lett.* 105(3): 037801.

Glaser, J., Hallatschek, O. & Kroy, K. (2008). Dynamic structure factor of a stiff polymer in a glassy solution., *Eur. Phys. J. E, Soft Matter* 26(1-2): 123–36.

Goldstein, R. & Langer, S. (1995). Nonlinear Dynamics of Stiff Polymers, *Phys. Rev. Lett.* 75(6): 1094–1097.

Granek, R. (1997). From Semi-Flexible Polymers to Membranes: Anomalous Diffusion and Reptation, *J. Phys. II* 7(12): 1761–1788.

Hallatschek, O., Frey, E. & Kroy, K. (2005). Propagation and Relaxation of Tension in Stiff Polymers, *Phys. Rev. Lett.* 94(7): 077804.

Hallatschek, O., Frey, E. & Kroy, K. (2007a). Tension dynamics in semiflexible polymers. I. Coarse-grained equations of motion, *Phys. Rev. E: Stat., Nonlinear, Soft Matter Phys.* 75(3): 031905.

Hallatschek, O., Frey, E. & Kroy, K. (2007b). Tension dynamics in semiflexible polymers. II. Scaling solutions and applications, *Phys. Rev. E: Stat., Nonlinear, Soft Matter Phys.* 75(3): 031906.

Hartwell, L. H., Hopfield, J. J., Leibler, S. & Murray, A. W. (1999). From molecular to modular cell biology, *Nature* 402(6761 Suppl): C47–52.

He, J., Viamontes, J. & Tang, J. (2007). Counterion-Induced Abnormal Slowdown of F-Actin Diffusion across the Isotropic-to-Nematic Phase Transition, *Phys. Rev. Lett.* 99(6): 068103.

Head, D., Levine, A. & MacKintosh, F. (2003). Deformation of Cross-Linked Semiflexible Polymer Networks, *Phys. Rev. Lett.* 91(10): 108102.

Heussinger, C., Bathe, M. & Frey, E. (2007). Statistical Mechanics of Semiflexible Bundles of Wormlike Polymer Chains, *Phys. Rev. Lett.* 99(4): 048101.

Heussinger, C. & Frey, E. (2006a). Floppy Modes and Nonaffine Deformations in Random Fiber Networks, *Phys. Rev. Lett.* 97(10): 105501.

Heussinger, C. & Frey, E. (2006b). Stiff Polymers, Foams, and Fiber Networks, *Phys. Rev. Lett.* 96(1): 017802.

Hinner, B., Tempel, M., Sackmann, E., Kroy, K. & Frey, E. (1998). Entanglement, Elasticity, and Viscous Relaxation of Actin Solutions, *Phys. Rev. Lett.* 81(12): 2614–2617.

Hinsch, H. & Frey, E. (2009). Conformations of entangled semiflexible polymers: entropic trapping and transient non-equilibrium distributions, *ChemPhysChem* 10(16): 2891–9.

Hinsch, H., Wilhelm, J. & Frey, E. (2007). Quantitative tube model for semiflexible polymer solutions, *Eur. Phys. J. E, Soft Matter* 24(1): 35–46.

Hiraiwa, T. & Ohta, T. (2008). Viscoelastic Behavior of a Single Semiflexible Polymer Chain, *J. Phys. Soc. Jpn.* 77(2): 023001.

Hiraiwa, T. & Ohta, T. (2009). Viscoelasticity of a Single Semiflexible Polymer Chain, *Macromolecules* 42(19): 7553–7562.

Hoffman, B. D. & Crocker, J. C. (2009). Cell mechanics: dissecting the physical responses of cells to force, *Annu. Rev. Biomed. Eng.* 11: 259–88.

Hoffman, B. D., Massiera, G., Van Citters, K. M. & Crocker, J. C. (2006). The consensus mechanics of cultured mammalian cells, *Proc. Natl. Acad. Sci. U. S. A.* 103(27): 10259–64.

Huisman, E., Storm, C. & Barkema, G. (2008). Monte Carlo study of multiply crosslinked semiflexible polymer networks, *Phys. Rev. E: Stat., Nonlinear, Soft Matter Phys.* 78(5): 051801.

Humphrey, D., Duggan, C., Saha, D., Smith, D. & Käs, J. (2002). Active fluidization of polymer networks through molecular motors, *Nature* 416(6879): 413–6.

Isambert, H. & Maggs, A. C. (1996). Dynamics and Rheology of Actin Solutions, *Macromolecules* 29(3): 1036–1040.

Isambert, H., Venier, P., Maggs, A., Fattoum, A., Kassab, R., Pantaloni, D. & Carlier, M. (1995). Flexibility of Actin Filaments Derived From Thermal Fluctuations, *J. Biol. Chem.* 270(19): 11437-11444.

Käs, J., Strey, H. & Sackmann, E. (1994). Direct imaging of reptation for semiflexible actin filaments, *Nature* 368: 226–229.

Kasza, K. E., Rowat, A. C., Liu, J., Angelini, T. E., Brangwynne, C. P., Koenderink, G. H. & Weitz, D. A. (2007). The cell as a material, *Curr. Opin. Cell Biol.* 19(1): 101–7.

Kirschner, M. & Gerhart, J. (1998). Evolvability, *Proc. Natl. Acad. Sci. USA* 95: 8420–8427.

Koenderink, G., Atakhorrami, M., MacKintosh, F. & Schmidt, C. (2006). High-Frequency Stress Relaxation in Semiflexible Polymer Solutions and Networks, *Phys. Rev. Lett.* 96(13): 138307.

Koenderink, G. H., Dogic, Z., Nakamura, F., Bendix, P. M., MacKintosh, F. C., Hartwig, J. H., Stossel, T. P. & Weitz, D. A. (2009). An active biopolymer network controlled by molecular motors, *Proc. Natl. Acad. Sci. U. S. A.* 106(36): 15192–7.

Kollmannsberger, P. (2009). *Nonlinear microrheology of living cells*, PhD thesis.

Kratky, O. & Porod, G. (1949). Röntgenuntersuchung gelöster Fadenmoleküle, *Rec. Trav. Chim. Pays-Bas* 68: 1105–1123.

Kroy, K. (2006). Elasticity, dynamics and relaxation in biopolymer networks, *Curr. Opin. Coll. Interface Sci.* 11(1): 56–64.

Kroy, K. (2008). Dynamics of wormlike and glassy wormlike chains, *Soft Matter* 4(12): 2323 – 2330.

Kroy, K. & Frey, E. (1996). Force-Extension Relation and Plateau Modulus for Wormlike Chains, *Phys. Rev. Lett.* 77(2): 306–309.

Kroy, K. & Frey, E. (1997). Dynamic scattering from solutions of semiflexible polymers, *Phys. Rev. E: Stat., Nonlinear, Soft Matter Phys.* 55(3): 3092–3101.

Kroy, K. & Glaser, J. (2007). The glassy wormlike chain, *New J. Phys.* 9(11): 416–416.

Kroy, K. & Glaser, J. (2009). Rheological redundancy - from polymers to living cells, *AIP Conf. Proc.* 1151: 52–55.

Landau, L. & Lifshitz, E. (1980). *Statistical Physics, Third Edition, Part 1: Volume 5 (Course of Theoretical Physics, Volume 5),* Butterworth-Heinemann, Oxford.

Lau, A., Hoffman, B., Davies, A., Crocker, J. & Lubensky, T. (2003). Microrheology, Stress Fluctuations, and Active Behavior of Living Cells, *Phys. Rev. Lett.* 91(19):198101

Lieleg, O. & Bausch, A. (2007). Cross-linker unbinding and self-similarity in bundled cytoskeletal networks, *Phys. Rev. Lett.* 99(15): 158105.

Lieleg, O., Claessens, M., Luan, Y. & Bausch, A. (2008). Transient binding and dissipation in cross-linked actin networks, *Phys. Rev. Lett.* 101(10): 108101.

Lieleg, O., Claessens, M. M. A. E. & Bausch, A. R. (2010). Structure and dynamics of crosslinked actin networks, *Soft Matter* 6(2): 218-225.

Lin, Y., Yao, N., Broedersz, C., Herrmann, H., MacKintosh, F. & Weitz, D. (2010). Origins of Elasticity in Intermediate Filament Networks, *Phys. Rev. Lett.* 104(5): 58101.

Liu, A. P. & Fletcher, D. A. (2009). Biology under construction: in vitro reconstitution of cellular function, *Nat. Rev. Mol. Cell. Biol.* 10(9): 644–50.

Liu, J., Koenderink, G., Kasza, K., MacKintosh, F. & Weitz, D. (2007). Visualizing the Strain Field in Semiflexible Polymer Networks: Strain Fluctuations and Nonlinear Rheology of F-Actin Gels, *Phys. Rev. Lett.* 98(19): 198304.

MacKintosh, F. C. (2006). *Elasticity and dynamics of cytoskeletal filaments and their networks*, Taylor & Francis, London, chapter 8, pp. 139–155.

MacKintosh, F. C., Käs, J. & Janmey, P. A. (1995). Elasticity of Semiflexible Biopolymer Networks, *Phys. Rev. Lett.* 75(24): 4425–4428.

MacKintosh, F. C. & Schmidt, C. F. (2010). Active cellular materials, *Curr. Opin. Cell Biol.* 22(1): 29–35.

Marko, J. & Siggia, E. (1995). Stretching DNA, *Macromolecules* 28(26): 8759–8770.

Mizuno, D., Bacabac, R., Tardin, C., Head, D. & Schmidt, C. (2009). High-Resolution Probing of Cellular Force Transmission, *Phys. Rev. Lett.* 102(16): 168102.

Mizuno, D., Tardin, C., Schmidt, C. F. & Mackintosh, F. C. (2007). Nonequilibrium mechanics of active cytoskeletal networks, *Science* 315(5810): 370–3.

Morse, D. C. (1998a). Viscoelasticity of concentrated isotropic solutions of semiflexible polymers. 1. Model and stress tensor, *Macromolecules* 31(20): 7030–7043.

Morse, D. C. (1998b). Viscoelasticity of Concentrated Isotropic Solutions of Semiflexible Polymers. 2. Linear Response, *Macromolecules* 31(20): 7044–7067.

Morse, D. C. (1998c). Viscoelasticity of tightly entangled solutions of semiflexible polymers, *Phys. Rev. E: Stat., Nonlinear, Soft Matter Phys.* 58(2): R1237–R1240.

Morse, D. C. (1999). Viscoelasticity of Concentrated Isotropic Solutions of Semiflexible Polymers. 3. Nonlinear Rheology, *Macromolecules* 32: 5934–5943.

Morse, D. C. (2001). Tube diameter in tightly entangled solutions of semiflexible polymers, *Phys. Rev. E: Stat., Nonlinear, Soft Matter Phys.* 63(3): 031502.

Munk, T., Hallatschek, O., Wiggins, C. & Frey, E. (2006). Dynamics of semiflexible polymers in a flow field, *Phys. Rev. E: Stat., Nonlinear, Soft Matter Phys.* 74(4): 041911.

Obermayer, B. & Frey, E. (2009). Tension dynamics and viscoelasticity of extensible wormlike chains, *Phys. Rev. E: Stat., Nonlinear, Soft Matter Phys.* 80(4): 040801(R).

Obermayer, B. & Hallatschek, O. (2007). Coupling of Transverse and Longitudinal Response in Stiff Polymers, *Phys. Rev. Lett.* 99(9): 098302.

Obermayer, B., Hallatschek, O., Frey, E. & Kroy, K. (2007). Stretching dynamics of semiflexible polymers, *Eur. Phys. J. E, Soft Matter* 23(4): 375–88.

Obermayer, B., Möbius, W., Hallatschek, O., Frey, E. & Kroy, K. (2009). Freely relaxing polymers remember how they were straightened, *Phys. Rev. E: Stat., Nonlinear, Soft Matter Phys.* 79(2): 021804.

Odijk, T. (1983). On the Statistics and Dynamics of Confined or Entangled Stiff Polymers, *Macromolecules* 1344(16): 1340–1344.

Onck, P., Koeman, T., van Dillen, T. & van Der Giessen, E. (2005). Alternative Explanation of Stiffening in Cross-Linked Semiflexible Networks, *Phys. Rev. Lett.* 95(17): 178102.

Ostermeir, K., Alim, K. & Frey, E. (2010). Buckling of stiff polymer rings in weak spherical confinement, *Phys. Rev. E: Stat., Nonlinear, Soft Matter Phys.* 81(6): 061802.

Pasquali, M., Shankar, V. & Morse, D. (2001). Viscoelasticity of dilute solutions of semiflexible polymers, *Phys. Rev. E: Stat., Nonlinear, Soft Matter Phys.* 64(2): 020802(R).

Ramanathan, S. & Morse, D. C. (2007). Simulations of dynamics and viscoelasticity in highly entangled solutions of semiflexible rods, *Phys. Rev. E: Stat., Nonlinear, Soft Matter Phys.* 76(1): 010501(R).

Romanowska, M., Hinsch, H., Kirchgeßner, N., Giesen, M., Degawa, M., Hoffmann, B., Frey, E. & Merkel, R. (2009). Direct observation of the tube model in F-actin solutions: Tube dimensions and curvatures, *Europhys. Lett.* 86(2): 26003.

Saitô, N., Takahashi, K. & Yunoki, Y. (1967). The Statistical Mechanical Theory of Stiff Chains, *J. Phys. Soc. Jpn.* 22(1): 219–226.

Schmoller, K., Lieleg, O. & Bausch, A. (2008). Cross-Linking Molecules Modify Composite Actin Networks Independently, *Phys. Rev. Lett.* 101(11): 118102.

Schopferer, M., Bär, H., Hochstein, B., Sharma, S., Mücke, N., Herrmann, H. & Willenbacher, N. (2009). Desmin and vimentin intermediate filament networks: their viscoelastic properties investigated by mechanical rheometry, *J. Mol. Biol.* 388(1): 133–43.

Schweizer, K., Fuchs, M., Szamel, G., Guenza, M. & Tang, H. (1997). Polymer-mode-coupling theory of the slow dynamics of entangled macromolecular fluids, *Macromol. Theory Simul.* 6: 1037–1117.

Schwille, P. & Diez, S. (2009). Synthetic biology of minimal systems, *Crit. Rev. Biochem. Mol. Biol.* 44(4): 223.242.

Seifert, U., Wintz, W. & Nelson, P. (1996). Straightening of Thermal Fluctuations in Semiflexible Polymers by Applied Tension, *Phys. Rev. Lett.* 77(27): 5389–5392.

Semenov, A. N. (1986). Dynamics of Concentrated Solutions of Rigid-chain Polymers Part 1. -Brownian Motion of Persistent Macromolecules in Isotropic Solution, *J. Chem. Soc., Faraday Trans.* 82(2): 317-329.

Semmrich, C., Larsen, R. J. & Bausch, A. R. (2008). Nonlinear mechanics of entangled F-actin solutions, *Soft Matter* 4(8): 1675-1680.

Semmrich, C., Storz, T., Glaser, J., Merkel, R., Bausch, A. R. & Kroy, K. (2007). Glass transition and rheological redundancy in F-actin solutions, *Proc. Natl. Acad. Sci. U. S. A.* 104(51): 20199–203.

Sollich, P., Lequeux, F., Hébraud, P. & Cates, M. (1997). Rheology of Soft Glassy Materials, *Phys. Rev. Lett.* 78(10): 2020–2023.

Storm, C., Pastore, J., MacKintosh, F., Lubensky, T. & Janmey, P. (2005). Nonlinear elasticity in biological gels, *Nature* 435(7039): 191.194.

Stricker, J., Falzone, T. & Gardel, M. L. (2010). Mechanics of the F-actin cytoskeleton, *J. Biomech.* 43(1): 9–14.

Tassieri, M., Evans, R. M. L., Barbu-Tudoran, L., Khan, G. N., Trinick, J. & Waigh, T. A. (2008). Dynamics of semi-flexible polymer solutions in the highly entangled regime, *Phys. Rev. Lett.* 101: 198301.

Tharmann, R., Claessens, M. & Bausch, A. (2007). Viscoelasticity of Isotropically Cross-Linked Actin Networks, *Phys. Rev. Lett.* 98(8): 088103.

Trepat, X., Deng, L., An, S. S., Navajas, D., Tschumperlin, D. J., Gerthoffer, W. T., Butler, J. P. & Fredberg, J. J. (2007). Universal physical responses to stretch in the living cell, *Nature* 447(7144): 592–5.

Trepat, X., Lenormand, G. & Fredberg, J. J. (2008). Universality in cell mechanics, *Soft Matter* 4(9): 1750.

Tskhovrebova, L., Trinick, J., Sleep, J. & Simmons, R. (1997). Elasticity and unfolding of single molecules of the giant muscle protein titin, *Nature* 387: 308–312.

Uchida, N., Grest, G. S. & Everaers, R. (2008). Viscoelasticity and primitive path analysis of entangled polymer liquids: from F-actin to polyethylene, *J. Chem. Phys.* 128(4): 044902.

Vaca Chávez, F. & Saalwächter, K. (2010). NMR Observation of Entangled Polymer Dynamics: Tube Model Predictions and Constraint Release, *Phys. Rev. Lett.* 104(19): 198305.

Vincent, R., Pinder, D., Hemar, Y. & Williams, M. (2007). Microrheological studies reveal semiflexible networks in gels of a ubiquitous cell wall polysaccharide, *Phys. Rev. E: Stat., Nonlinear, Soft Matter Phys.* 76(3): 031909.

Wagner, B., Tharmann, R., Haase, I., Fischer, M. & Bausch, A. R. (2006). Cytoskeletal polymer networks: the molecular structure of cross-linkers determines macroscopic properties, *Proc. Natl. Acad. Sci. U. S. A.* 103(38): 13974–8.

Wang, B., Guan, J., Anthony, S. M., Bae, S. C., Schweizer, K. S. & Granick, S. (2010). Confining Potential when a Biopolymer Filament Reptates, *Phys. Rev. Lett.* 104(11): 118301.

Wilhelm, J. & Frey, E. (1996). Radial Distribution Function of Semiflexible Polymers, *Phys. Rev. Lett.* 77(12): 2581–2584.

Wilhelm, J. & Frey, E. (2003). Elasticity of Stiff Polymer Networks, *Phys. Rev. Lett.* 91(10): 108103.

Wolff, L., Fernandez, P. & Kroy, K. (2010). Inelastic mechanics of sticky biopolymer networks, *New J. Phys.* 12(5): 053024.

Yamakawa, H. (1971). *Modern Theory of Polymer Solutions*, Harper & Row, New York.

Zhou, Q. & Larson, R. (2006). Direct calculation of the tube potential confining entangled polymers, *Macromolecules* 39(19): 6737–6743.
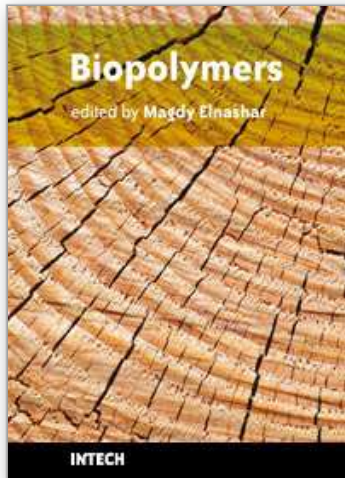
**Biopolymers**

Edited by Magdy Elnashar

Biopolymers are polymers produced by living organisms. Cellulose, starch, chitin, proteins, peptides, DNA and RNA are all examples of biopolymers. This book comprehensively reviews and compiles information on biopolymers in 30 chapters. The book covers occurrence, synthesis, isolation and production, properties and applications, modification, and the relevant analysis methods to reveal the structures and properties of some biopolymers. This book will hopefully be of help to many scientists, physicians, pharmacists, engineers and other experts in a variety of disciplines, both academic and industrial. It may not only support research and development, but be suitable for teaching as well.

**How to reference**

In order to correctly reference this scholarly work, feel free to copy and paste the following:

Jens Glaser and Klaus Kroy (2010). Fluctuations of Stiff Polymers and Cell Mechanics, Biopolymers, Magdy Elnashar (Ed.), ISBN: 978-953-307-109-1, InTech, Available from:
http://www.intechopen.com/books/biopolymers/fluctuations-of-stiff-polymers-and-cell-mechanics-

# INTECH
open science | open minds